Coherent generation and manipulation of stationary light pulses encoded in degrees of freedom of polarization and orbital angular momentum

Tianhui Qiu,[1,*] Hui Li,[2] and Min Xie[3]

[1]*School of Science, Qingdao University of Technology, Qingdao 266033, China*

[2]*Optoelectronic Materials and Technologies Engineering Laboratory of Shandong, College of Mathematical and Physical Sciences, Qingdao University of Science and Technology, Qingdao 266061, China*

[3]*College of Physics and Communication Electronics, and Center for Quantum Science and Technology, Jiangxi Normal University, Nanchang 330022, China*

(Received 6 January 2019; revised manuscript received 6 May 2019; published 23 July 2019)

We propose a double-M system of cold atoms for realizing the reversible storage and manipulation of signal fields encoded in degrees of freedom (DOFs) of polarization and orbital angular momentum (OAM). By employing two pairs of counterpropagating controlling fields, we show that the system exhibits dark state polaritons relating to the polarization and propagation direction of the light fields. Through the active operation of the controlling fields in time, stationary light pulses with polarizations and OAM information can be generated due to the tight coupling and balanced competition between the retrieved signal fields, and can be manipulated coherently and all-optically. Another advantage of our proposed scheme is that the two polarization components of the signal field can be decoupled and thus be independently retrieved from the atomic ensemble, and then the scheme can be employed to realize polarization-dependent beam splitting. Such a multiple DOF-dependent scheme could pave the way toward quantum nonlinear optics without a cavity, and could greatly enhance the tunability and capacity for both classical and quantum information processing.

DOI: 10.1103/PhysRevA.100.013844

I. INTRODUCTION

The reversible storage and coherent manipulation of light have attracted significant interest in recent decades and are expected to play important roles in both the all-optical classical and the quantum information systems. For example, in long-distance quantum communication, quantum memories are the most important component of the quantum repeaters [1,2]. For realizing practical light storage, several mechanisms, such as electromagnetically induced transparency (EIT) [3–7], atomic frequency combs [8,9], Raman schemes [10,11], and the gradient echo technique [12–15], have been proposed. Because of the inherent determinacy, the EIT-based scheme described in terms of the dark-state polariton (DSP) [16] seems a good candidate and thus has attracted much attention since its discovery. By the adiabatic operation of the traveling-wave controlling field in time, researchers have experimentally demonstrated the storage of classical light pulses [3,17,18], single-photon states, and squeezed vacuum states in a series of impressive experiments [19,20]. The entangled state of light has also been mapped into and out of an EIT quantum memory by using two spatially separated interaction regions [21]. By substituting the standing-wave controlling field for the traveling-wave controlling field in the EIT medium, André and Lukin first proposed the concept of stationary light pulses (SLPs) in 2002 [22]. Soon, the phenomenon was observed in ^{87}Rb vapor by Bajcsy *et al.* in 2003 [23]. SLPs, the duration of which is no longer restricted by the atomic spin coherence, can remarkably increase the interaction time between light and atoms, and can find important potential applications in the fields of low-light-level nonlinear optics and photonic quantum information processing without a cavity [24]. Because of the significant advantages of the SLPs, a lot of meaningful results have been achieved in the candidate media [25–31], while the presence of many higher-order Fourier components of spin coherence and optical coherence in the typical three-level Λ system of cold atoms makes SLPs experience fast decay and diffusion. For attaining robust SLPs, schemes implementing in a hot atomic vapor with large Doppler broadening [23] or employing counterpropagating controlling fields with different frequencies [27–30] have been proposed.

For realizing large-scale quantum networks in future applications, reversible storage and manipulation of the higher-dimensional states of light has received much attention. Recently, multimode transverse images have been stored in an atomic ensemble or in a cryogenically cooled doped crystal via EIT [32–34]. The orbital angular momentum (OAM) of a photon with inherent infinite dimension has proven to be an outstanding degree of freedom (DOF) for carrying high-dimensional states [35,36]. The coherent and nonlinear interaction of light beams carrying OAMs with atomic systems has been reported previously using different experimental schemes [37–39], and tremendous developments have also been realized in the reversible storage of OAM states [40,41]. For further meeting the requirements of quantum information science, an experimental scheme for storing a single photon carrying OAMs based on EIT in a cold atomic ensemble has been proposed [42]. The storage of a photon pair entangled in OAM space has also been implemented

*qth_009@126.com

experimentally through the Raman protocol in a cold atomic ensemble [43]. Very recently, in order to make full use of the advantages of different DOFs and significantly improve the communication capacity of quantum memories and quantum channels, quantum memories utilizing more than one DOF simultaneously have been proposed [44–46]. Entanglement in multiple DOFs between two quantum memories has also been realized experimentally [47].

In this paper, through combining the DOFs of the polarization and OAM, we propose a double-M system of cold atoms for realizing multiple-DOF storage with high multimode capacity. By the active operation of the two pairs of counter-propagating controlling fields in time, we find that the system exhibits DSPs relating to the polarization and propagation direction of the light fields, and SLPs encoded in the DOFs of polarization and OAM can be generated and manipulated coherently. Another advantage of the proposed scheme is that the two polarization components of the signal fields can be decoupled and thus be independently retrieved from the atomic ensemble. Our results are expected to find applications in large-scale storage-based networks and advanced information processing architectures.

II. THEORETICAL MODEL AND EQUATIONS OF MOTION

We consider a medium of length L consisting of an ensemble of seven-level cold atoms in the double-M configuration as shown in Fig. 1(a). According to the polarizations of the input signal fields, the interaction of signal fields with the atomic ensemble separates into two classes of double-Λ systems, which are illustrated in Figs. 1(b) and 1(c). A weak signal field with left circular polarization E_{L+} of frequency ω_{L+} (or wave number k_{L+}) propagating in the $+\vec{z}$ direction is applied to the atomic transition $|1\rangle \rightarrow |3\rangle$, two strong controlling fields with π polarization E_{1+} of frequency ω_{1+} (or wave number k_{1+}) and E_{1-} of frequency ω_{1-} (or wave number k_{1-}) travel in the $+\vec{z}$ and $-\vec{z}$ direction, and are coupled to the atomic transitions $|2\rangle \rightarrow |3\rangle$ and $|2\rangle \rightarrow |4\rangle$, respectively. As a result of four-wave mixing, a weak signal field with left circular polarization E_{L-} propagating in the $-\vec{z}$ direction is expected to be generated on the transition from level $|4\rangle$ to level $|1\rangle$. The levels $|1\rangle$, $|2\rangle$, $|3\rangle$, and $|4\rangle$ form a four level double-Λ system as shown in Fig. 1(b). A weak signal field with right circular polarization E_{R+} of frequency ω_{R+} (or wave number k_{R+}) undergoes a process similar to that of the signal field E_{L+} except that it is applied to the transition $|1\rangle \rightarrow |6\rangle$, then a weak signal field with right circular polarization E_{R-} propagating in the $-\vec{z}$ direction is generated by four-wave mixing. The levels $|1\rangle$, $|5\rangle$, $|6\rangle$, and $|7\rangle$ coupled by two signal fields (E_{R+} and E_{R-}) and two strong controlling fields (E_{2+} and E_{2-} with π polarization) form the other four level double-Λ system as shown in Fig. 1(c). The two double-Λ systems share the same ground state $|1\rangle$, and can be employed for coherent generation and manipulation of SLPs with left and right circular polarizations. Such level structures can be realized in the $D1$ or $D2$ transitions of ^{87}Rb atoms.

The equations of motion for the signal fields with left (right) circular polarization $E_{L(R)\pm}$ in the medium are

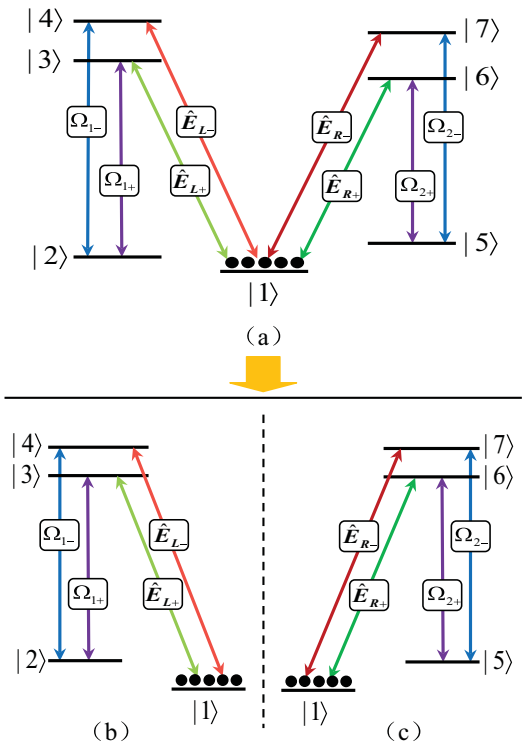

FIG. 1. (a) Schematic of a double-M linkage structure, which can be realized in the ^{87}Rb $D1$ or $D2$ transitions. (b), (c) Corresponding decompositions of atom-field interaction in (a) according to the polarizations of the signal fields [(b) for the left circular polarization, (c) for the right circular polarization].

governed by the Maxwell equations

$$\nabla^2 E_{L(R)\pm} - \frac{1}{c^2}\frac{\partial^2 E_{L(R)\pm}}{\partial t^2} = \frac{1}{\varepsilon_0 c^2}\frac{\partial^2 P_{L(R)\pm}}{\partial t^2}, \tag{1}$$

where $E_{L(R)\pm}$ is defined as $E_{L(R)\pm} = \mathcal{E}_{L(R)\pm} e^{i(\pm k_{L(R)\pm} z - \omega_{L(R)\pm} t)} +$ c.c. with the slowly varying envelope $\mathcal{E}_{L(R)\pm}$. $P_{L(R)\pm}$ is the polarization of the medium described by $P_{L(R)\pm} = \mathcal{P}_{L(R)\pm} e^{i(\pm k_{L(R)\pm} z - \omega_{L(R)\pm} t)} +$ c.c. with a slowly varying envelope $\mathcal{P}_{L(R)\pm}$. For the present system, $\mathcal{P}_{L+}$ ($\mathcal{P}_{L-}$) is related to the atomic transition $|1\rangle \rightarrow |3\rangle$ ($|1\rangle \rightarrow |4\rangle$) and can be expressed as $\mathcal{P}_{L+} = N d_{13}\rho_{31}$ ($\mathcal{P}_{L-} = N d_{14}\rho_{41}$), and $\mathcal{P}_{R+}$ ($\mathcal{P}_{R-}$) is related to the atomic transition $|1\rangle \rightarrow |6\rangle$ ($|1\rangle \rightarrow |7\rangle$) and can be expressed as $\mathcal{P}_{R+} = N d_{16}\rho_{61}$ ($\mathcal{P}_{R-} = N d_{17}\rho_{71}$), where ρ_{31} and ρ_{61} (ρ_{41} and ρ_{71}) are the relevant density matrix elements.

Under the slowly varying envelope approximation, the equations of motion for the signal fields $E_{L(R)\pm}$ can be reduced to

$$\begin{aligned}
&\frac{\partial \Omega_{L(R)+}}{\partial z} + \frac{1}{c}\frac{\partial \Omega_{L(R)+}}{\partial t} \\
&= \frac{i}{2k_{L(R)+}}\nabla_\perp^2 \Omega_{L(R)+} + i\frac{N d_{13(6)}^2 k_{L(R)+}}{2\varepsilon_0 \hbar}\rho_{3(6)1}, \\
&\frac{\partial \Omega_{L(R)-}}{\partial z} - \frac{1}{c}\frac{\partial \Omega_{L(R)-}}{\partial t} \\
&= -\frac{i}{2k_{L(R)-}}\nabla_\perp^2 \Omega_{L(R)-} - i\frac{N d_{14(7)}^2 k_{L(R)-}}{2\varepsilon_0 \hbar}\rho_{4(7)1},
\end{aligned} \tag{2}$$

where $\nabla_\perp^2 = \partial^2/\partial x^2 + \partial^2/\partial y^2$, $\Omega_{L(R)+} = \mathcal{E}_{L(R)+}d_{3(6)1}/2\hbar$, and $\Omega_{L(R)-} = \mathcal{E}_{L(R)-}d_{4(7)1}/2\hbar$. d_{kj} $(k \neq j)$ is the electric-dipole moment on the transition $|k\rangle \to |j\rangle$.

Without loss of generality, we assume that all the signal fields and the controlling fields are coupled to the corresponding atomic transitions resonantly. Then we can express the interaction Hamiltonian of the whole system in the dipole and rotating wave approximations as follows:

$$\begin{aligned} H = -\hbar[&\Omega_{L+}|3\rangle\langle 1| + \Omega_{L-}|4\rangle\langle 1| + \Omega_{1+}|3\rangle\langle 2| + \Omega_{1-}|4\rangle\langle 2| \\ &+ \Omega_{R+}|6\rangle\langle 1| + \Omega_{R-}|7\rangle\langle 1| + \Omega_{2+}|6\rangle\langle 5| + \Omega_{2-}|7\rangle\langle 5| \\ &+ \text{H.c.}], \end{aligned} \tag{3}$$

and $\Omega_{1\pm}$ and $\Omega_{2\pm}$ are the Rabi frequencies of the four applied controlling fields (see Fig. 1). From the interaction Hamiltonian (3), we can obtain the Liouville equations expanded into density matrix elements of the system under the assumption of weak signal fields. The reduced dynamic equations to the first order in the signal fields are shown as follows:

$$\begin{aligned} \frac{\partial \rho_{12}}{\partial t} &= -\gamma_{21}\rho_{12} - i\Omega_{1+}\rho_{13} - i\Omega_{1-}\rho_{14}, \\ \frac{\partial \rho_{13}}{\partial t} &= -\gamma_{31}\rho_{13} - i\Omega_{1+}^*\rho_{12} - i\Omega_{L+}^*, \\ \frac{\partial \rho_{14}}{\partial t} &= -\gamma_{41}\rho_{14} - i\Omega_{1-}^*\rho_{12} - i\Omega_{L-}^*, \\ \frac{\partial \rho_{15}}{\partial t} &= -\gamma_{51}\rho_{15} - i\Omega_{2+}\rho_{16} - i\Omega_{2-}\rho_{17}, \\ \frac{\partial \rho_{16}}{\partial t} &= -\gamma_{61}\rho_{16} - i\Omega_{2+}^*\rho_{15} - i\Omega_{R+}^*, \\ \frac{\partial \rho_{17}}{\partial t} &= -\gamma_{71}\rho_{17} - i\Omega_{2-}^*\rho_{15} - i\Omega_{R-}^*, \end{aligned} \tag{4}$$

where γ_{kj} is the decay rate of atomic coherence on transition $|k\rangle \leftrightarrow |j\rangle$. With Eqs. (2) and (4) in hand, we can examine the propagation dynamics of the signal fields encoded in the DOFs of polarization and OAM.

For intuitively revealing the reversible storage and manipulation of the signal fields with OAMs, the Rabi frequencies of the signal fields $\Omega_{L(R)\pm}$ are expanded as follows:

$$\Omega_{L(R)\pm}(r,t) = \sum_{m,n} \mathcal{L}^{mn}(r,\psi,z)\Omega_{L(R)\pm}^{mn}(z,t), \tag{5}$$

where $r = (x^2+y^2)^{1/2}$ and ψ are the radial coordinate and azimuthal angle in the framework of the cylindrical coordinate system, and $\Omega_{L(R)\pm}^{mn}(z,t)$ are expansion coefficients. The function $\mathcal{L}^{mn}(r,\psi,z)$ satisfies the equation $2ik_{L(R)\pm}\partial\mathcal{L}^{mn}(r,\psi,z)/\partial z + \nabla_\perp^2\mathcal{L}^{mn}(r,\psi,z) = 0$, which admits eigensolutions in the form of Laguerre-Gaussian $(\text{LG})_n^m$ modes with OAM $m\hbar$ along the z direction. If the diffraction effect of the system is small (i.e., z is large enough), the eigensolutions can be approximated by [48,49]

$$\mathcal{L}^{mn}(r,\psi) = \frac{C_{mn}}{\sqrt{w_0}}\left[\frac{\sqrt{2}r}{w_0}\right]^{|m|}\exp\left[-\frac{r^2}{w_0^2}\right]L_n^{|m|}\left[\frac{2r^2}{w_0^2}\right]\exp(im\psi), \tag{6}$$

where $C_{mn} = \sqrt{2^{|m|+1}n!/[\pi(|m|+n)!]}$ is the normalization constant, w_0 is the beam waist, $L_n^{|m|}$ are the generalized LG polynomials, and m and n are azimuthal and radial indices. The profiles of the $(\text{LG})_n^m$ modes show concentric rings, the number of which is determined by the mode index n. The mode index m is contained in the azimuthal phase term $\exp(im\psi)$, which gives rise to $|m|$ intertwined helical wave fronts. The handedness of these helixes is determined by the sign of m.

Based on the same basis used for the signal fields, the density matrix element ρ_{kj} can be conveniently expanded as follows:

$$\rho_{kj}(r,t) = \sum_{m,n}\mathcal{L}^{mn}(r,\psi)\rho_{kj}^{mn}(z,t), \tag{7}$$

where $\rho_{kj}^{mn}(z,t)$ is the expansion coefficient. Substituting Eqs. (5) and (7) into Eq. (2), we can obtain the equations for $\Omega_{L(R)\pm}^{mn}(z,t)$ as follows:

$$\begin{aligned} \frac{\partial\Omega_{L(R)+}^{mn}}{\partial z} + \frac{1}{c}\frac{\partial\Omega_{L(R)+}^{mn}}{\partial t} &= i\frac{Nd_{13(6)}^2 k_{L(R)+}}{2\varepsilon_0\hbar}\rho_{3(6)1}^{mn}, \\ \frac{\partial\Omega_{L(R)-}^{mn}}{\partial z} - \frac{1}{c}\frac{\partial\Omega_{L(R)-}^{mn}}{\partial t} &= -i\frac{Nd_{14(7)}^2 k_{L(R)-}}{2\varepsilon_0\hbar}\rho_{4(7)1}^{mn}. \end{aligned} \tag{8}$$

The form of Eqs. (8) is the same as the Maxwell wave equation describing the propagation dynamics of the general light pulses in the atomic ensemble. Thus, we can firmly believe that the present scheme can be used for coherent generation and manipulation of SLPs with OAMs.

If only the fields propagating in the $+\vec{z}$ direction ($\Omega_{L(R)+}$, $\Omega_{1(2)+}$) are applied, Eqs. (8) and the dynamic equations on $\rho_{kj}^{mn}(z,t)$ can be transformed into

$$\left(\frac{\partial}{\partial t} + v_{L(R)+}\frac{\partial}{\partial z}\right)\Psi_{L(R)+}^{mn}(z,t) = 0, \tag{9}$$

where $\Psi_{L(R)+}^{mn}(z,t) = \cos\theta_{L(R)+}(t)E_{L(R)+}^{mn} - \sin\theta_{L(R)+}(t)\sqrt{N}\rho_{12(5)}^{mn}$, with $\tan^2\theta_{L(R)+} = g_{L(R)+}^2 N/\Omega_{1(2)+}^2$ and $g_{L(R)+}^2 = \frac{d_{13(6)}^2\omega_{L(R)+}}{2\varepsilon_0\hbar}$, is the so-called DSP for the $(\text{LG})_n^m$ mode of the signal field with the left (right) circular polarization. It is shape preserving during propagation in the $+\vec{z}$ direction with the velocity $v_{L(R)+} = c\cos^2\theta_{L(R)+}$, which can become zero through switching off the controlling field $\Omega_{1(2)+}$ adiabatically.

If only the fields $\Omega_{L(R)-}$ and $\Omega_{1(2)-}$, which propagate in the $-\vec{z}$ direction, are applied, similar to the above derivation process, Eqs. (8) and the dynamic equations on $\rho_{kj}^{mn}(z,t)$ can be transformed into

$$\left(\frac{\partial}{\partial t} - v_{L(R)-}\frac{\partial}{\partial z}\right)\Psi_{L(R)-}^{mn}(z,t) = 0. \tag{10}$$

Equation (10) describes the shape-preserving propagation of DSP $\Psi_{L(R)-}^{mn}(z,t) = \cos\theta_{L(R)-}(t)E_{L(R)-}^{mn} - \sin\theta_{L(R)-}(t)\sqrt{N}\rho_{12(5)}^{mn}$ for the $(\text{LG})_n^m$ mode of the signal field with the left (right) circular polarization, which propagates in the $-\vec{z}$ direction with velocity $v_{L(R)-} = c\cos^2\theta_{L(R)-}$, where $\tan^2\theta_{L(R)-} = g_{L(R)-}^2 N/\Omega_{1(2)-}^2$, and $g_{L(R)-}^2 = \frac{d_{14(7)}^2\omega_{L(R)-}}{2\varepsilon_0\hbar}$.

In the case considered in the present paper, if only the signal field with left (right) circular polarization is input into the atomic ensemble, the two DSPs $\Psi_{L(R)+}^{mn}(z,t)$ and $\Psi_{L(R)-}^{mn}(z,t)$ can be simultaneously generated, and share the same atomic spin coherence $\rho_{12(5)}^{mn}$. Thus, this system can be

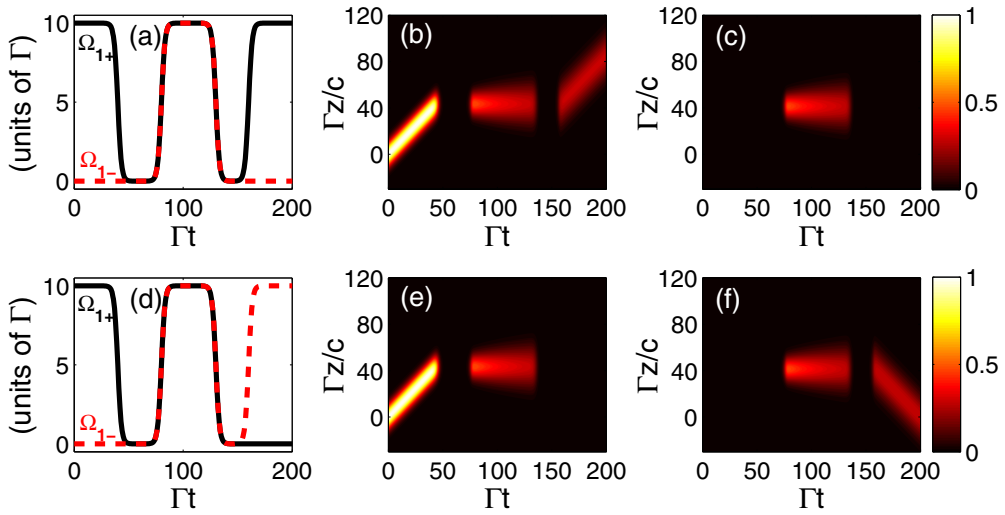

FIG. 2. Time evolution of the controlling fields Ω_{1+} (black solid curves) and Ω_{1-} (red dashed curves) in an adiabatic way (a), (d), and dynamic propagation and evolution of the signal fields with left circular polarization propagating in the $+\vec{z}$ (b), (e) and $-\vec{z}$ (c), (f) directions. The parameters are $\gamma_{31} = \gamma_{41} = \gamma_{61} = \gamma_{71} = 1.5\Gamma$, $\gamma_{21} = \gamma_{51} = 0.001\Gamma$, and $\Omega_1 = 10\Gamma$, where Γ is the population decay rate from the excited level to the ground level, and $\Gamma = 5.75$ MHz. $\lambda_{H\pm} = \lambda_{1\pm} = 795$ nm.

used for generation and manipulation of SLPs encoded in the DOFs of left (right) circular polarization and OAM by actively operating the controlling fields $\Omega_{1(2)\pm}$ in time. If the mixed signal field (including the fields with the left and right circular polarizations) is input into the atomic ensemble, based on the above analysis, left and right circular polarization encoded SLPs can be generated simultaneously. By cooperatively operating all the four controlling fields $\Omega_{1(2)\pm}$ adiabatically, the retrieved signal fields with left and right circular polarizations can be separated spatially. Thus, this scheme can be also used as a coherent storage-based polarization beam splitter.

III. RESULTS AND DISCUSSION

Now, we use numerical simulation to examine the purposes of the proposed scheme, i.e., coherent generation and manipulation of SLPs encoded in the DOFs of polarization and OAM by accurately switching on and off the controlling fields $\Omega_{1(2)\pm}$ in time.

A. Generation and manipulation of SLPs with left or right circular polarization

First, we consider the simplest case, i.e., only the signal field with left circular polarization Ω_{L+} is input into the atomic ensemble, where all the atoms have been pumped into the level $|1\rangle$. According to the above analysis, the effective schematic of atom-field interaction is shown in Fig. 1(b). To generate the SLPs on demand, we assume that the counter-propagating controlling fields Ω_{1+} and Ω_{1-} vary regularly in terms of the formulas $\Omega_{1+} = \Omega_1[1 - 0.5\tanh\frac{t-t_1}{t_s} + 0.5\tanh\frac{t-t_2}{t_s} - 0.5\tanh\frac{t-t_3}{t_s} + 0.5\tanh\frac{t-t_4}{t_s}]$ and $\Omega_{1-} = \Omega_1[0.5\tanh\frac{t-t_2}{t_s} - 0.5\tanh\frac{t-t_3}{t_s}]$. The varying curves of both the controlling fields are shown in Fig. 2(a). As the signal field Ω_{L+} and the controlling field Ω_{1+} enter the atomic medium, according to the DSP theory, the information carried by the signal field Ω_{L+} is mapped into the atomic spin coherence ρ_{12} when the controlling field is switched off at $t = t_1$ ($\Gamma t_1 = 40$). After a decent interval, at $t = t_2$ ($\Gamma t_2 = 80$), the controlling fields Ω_{1+} and Ω_{1-} with the same intensity are switched on, then two signal fields Ω_{s+} and Ω_{s-} with the same intensity propagating in the opposite directions are retrieved from the atomic spin coherence ρ_{12} determinately. As the result of the tight coupling and balanced competition between the two retrieved signal fields, SLPs are generated [see Figs. 2(b) and 2(c)]. The SLPs can also be released by the reverse process, i.e., first switching off both the controlling fields at $t = t_3$ ($\Gamma t_3 = 130$) to transfer the information carried by the SLPs into the atomic spin coherence ρ_{12} again, then switching on the controlling field Ω_{1+} at $t = t_4$ ($\Gamma t_4 = 160$) to retrieve the signal field Ω_{L+} propagating in the $+\vec{z}$ direction [see Figs. 2(b) and 2(c)].

There are two facts that need to be emphasized. The first concerns what happens if the two controlling fields Ω_{1+} and Ω_{1-} take the forms $\Omega_{1+} = \Omega_1[0.5 - 0.5\tanh\frac{t-t_1}{t_s} + 0.5\tanh\frac{t-t_2}{t_s} - 0.5\tanh\frac{t-t_3}{t_s}]$ and $\Omega_{1-} = \Omega_1[0.5 + 0.5\tanh\frac{t-t_2}{t_s} - 0.5\tanh\frac{t-t_3}{t_s} + 0.5\tanh\frac{t-t_4}{t_s}]$, respectively. The varying curves of both the controlling fields are shown in Fig. 2(d). Compared to the above case, the only difference is that, at $t = t_4$, the controlling field Ω_{1-} is switched on and Ω_{1+} keeps closed, then only the signal field Ω_{L-} propagating in the $-\vec{z}$ direction is retrieved [see Figs. 2(e) and 2(f)]. Second, as the signal field with right circular polarization E_{R+} is input into the atomic ensemble, it undergoes a process similar to that of the signal field E_{L+} on the basis of the varying of the controlling fields Ω_{2+} and Ω_{2-}. In other words, the proposed scheme can be employed for the reversible storage and manipulation of the signal fields with left and right circular polarizations independently.

B. Storage-based polarization beam splitter

Second, we assume that the mixed signal field is input into the atomic ensemble, and the two polarization components

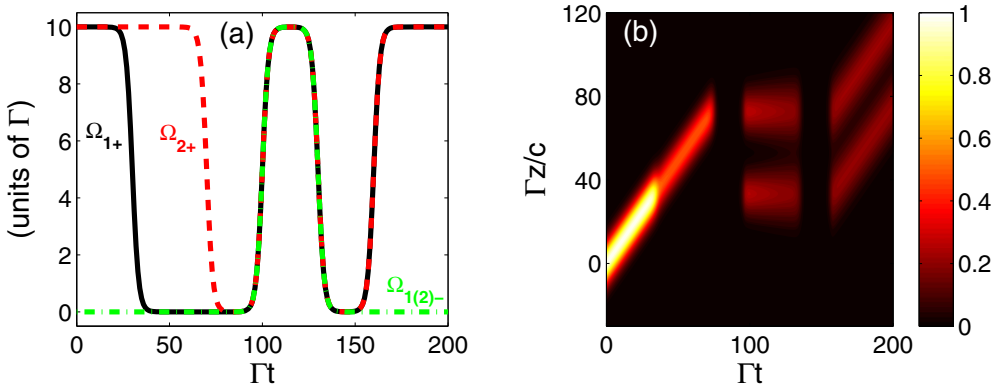

FIG. 3. (a) Time evolution of the controlling fields Ω_{1+} (black solid curve), Ω_{2+} (red dashed curve), and $\Omega_{1(2)-}$ (green dash-dotted curve) in an adiabatic way. (b) Dynamic propagation and evolution of the mixed signal fields propagating in the $+\vec{z}$ direction, where the controlling fields $\Omega_{1\pm}$ and $\Omega_{2\pm}$ vary in accordance with Fig. 3(a). The other parameters are the same as in Fig. 2.

of the mixed signal field are equal in intensity. Apparently, in view of the above results, the signal field with left (right) circular polarization is coupled to the atomic transition $|1\rangle \rightarrow |3\rangle$ ($|1\rangle \rightarrow |6\rangle$), and evolves on the basis of the varying of the controlling fields $\Omega_{1\pm}$ ($\Omega_{2\pm}$). Thus, we propose two schemes for realizing the spatial separation of the two polarization components of the mixed signal field by cooperatively operating all the four controlling fields $\Omega_{1(2)\pm}$.

In scheme 1, the controlling fields are operated according to Fig. 3(a). Because the controlling fields Ω_{1+} are switched off earlier than the controlling fields Ω_{2+} when they are turned off at the first time for storing the information carried by the mixed signal field into the atomic spin coherence, the information carried by the two polarization components of the mixed signal field will be stored in different locations of the atomic medium [see Fig. 3(b)]. In the next whole process, the variety of the controlling field Ω_{1+} (Ω_{1-}) is the same as that of the controlling field Ω_{2+} (Ω_{2-}). The two polarization components of the mixed signal field will evolve in exactly the same regularity (propagating in the same velocity and direction), and are separated spatially in the following process [see Fig. 3(b)]. The separated distance is proportional to the difference in time of switching off the two controlling fields (Ω_{1+} and Ω_{2+}) at the first time. It should be noted that the two polarization components of the mixed signal field can also be separated spatially by turning on the controlling fields Ω_{1+} and Ω_{2+} at different times when they are turned on at the second time for retrieving the information stored in the atomic spin coherence. Certainly, the two cases can be applied to one process for flexibly modulating the separated distance between the two polarization components. In the scheme, although the signal fields with left and right circular polarizations can be retrieved from the atomic medium at different times, they still propagate in the same direction.

In scheme 2, we assume that the controlling fields Ω_{1+} (Ω_{2+}) and Ω_{1-} (Ω_{2-}) vary along the black solid and the red dashed curves in Fig. 2(a) [Fig. 2(d)]. Obviously, the evolutionary process of the two polarization components of the mixed signal field is exactly the same before $t = t_4$ (see Fig. 4). Subsequently, the controlling fields Ω_{1+} (Ω_{2-}) are switched on, then the signal field with left (right) circular polarization propagating in the $+\vec{z}$ ($-\vec{z}$) direction is released. Compared to scheme 1, the two components of the mixed signal field can be retrieved at the same time or at different times, and the retrieved signal fields with left and right circular polarizations can propagate in the same direction or in opposite directions (see Fig. 4). Both the two schemes can be employed as a coherent storage-based polarization beam splitter, and can find potential applications in many fields.

C. Reversible storage and manipulation of signal fields with OAMs

Then, coherent generation and manipulation of SLPs with left circular polarization and OAMs is investigated by numerical simulation. We assume that the Rabi frequencies of the controlling fields Ω_{1+} and Ω_{1-} vary in accordance with Fig. 2(a). The intensity distributions of the signal field Ω_{L+} with the transversal LG modes in the x-y plane before and after the storage are shown in Fig. 5. Figure 5(a) (for $\Gamma t = 0$) gives the intensity pattern for the superposition of a set of LG modes $[(\mathrm{LG})_0^0+(\mathrm{LG})_0^4+(\mathrm{LG})_0^{-4}+(\mathrm{LG})_2^0]$ before the storage,

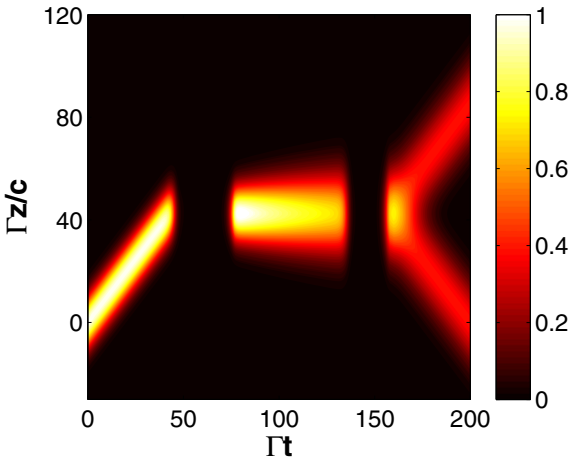

FIG. 4. Dynamic propagation and evolution of the mixed signal fields, where the controlling fields $\Omega_{1\pm}$ [$\Omega_{2\pm}$] vary in accordance with Fig. 2(a) [Fig. 2(d)]. The other parameters are the same as in Fig. 2.

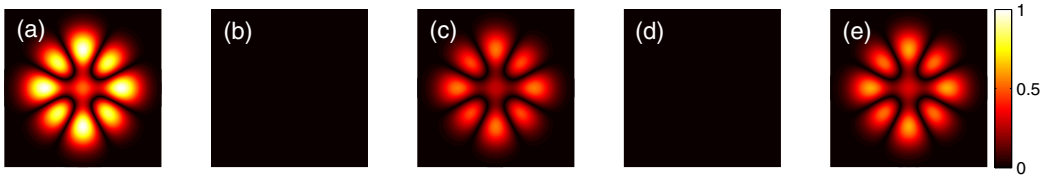

FIG. 5. Reversible storage and manipulation of signal fields with left circular polarization and OAM information, where the controlling fields $\Omega_{1\pm}$ vary in accordance with Fig. 2(a). The normalized intensity patterns for the superposition of LG modes $[(\mathrm{LG})_0^0+(\mathrm{LG})_0^4+(\mathrm{LG})_0^{-4}+(\mathrm{LG})_2^0]$ at time $\Gamma t = 0$ (a), 60 (b), 100 (c), 145 (d), and 200 (e), respectively. The size of the patterns is 3×3 mm^2. The other parameters are the same as in Fig. 2.

Fig. 5(c) (for $\Gamma t = 100$) gives the patterns of the generated SLPs, and Fig. 5(e) (for $\Gamma t = 200$) gives the retrieved pattern. The patterns of Figs. 5(b) and 5(d) are obtained as both the controlling fields are switched off completely, then we can find that the optical components disappear because the information of the pattern has been mapped into the atomic spin coherence ρ_{12}. The retrieved pattern in the Fig. 5(e) is obtained at the exit of the medium. If only the controlling field Ω_{1-} is switched on in the time $t = t_4$, the pattern can also be released from the medium entrance. It should be noted that the phase distribution of the LG modes, which carry OAM information, can also be reversibly stored. Compared to the reduction of the amplitude of the retrieved signal field, the phase distribution is unaffected during this process. According to the above obtained results, this scheme is also suitable for the signal field with right circular polarization and OAMs by actively operating the controlling fields $\Omega_{2\pm}$ in time, and can be employed as a coherent storage-based polarization beam splitter for the signal field encoded in the DOFs of polarization and OAM.

D. Reversible storage and manipulation of signal fields with nonuniform controlling fields

In the above discussion, we assume that the controlling fields $\Omega_{1\pm}$ and $\Omega_{2\pm}$ are spatially uniform, and vary with time only. Then, the different $(\mathrm{LG})_n^m$ modes are independent of each other in the whole process. However, in the practical experiments, the controlling fields are usually radially symmetric, and can be expressed in the form $\Omega_{1(2)\pm}(r,t) = R_{1(2)\pm}(r)T_{1(2)\pm}(t)$, where $R_{1(2)\pm}(r)$ is the spatial distribution function, and $T_{1(2)\pm}(t)$ is the time-dependent amplitude. Under the condition, the reduced dynamic equations for ρ_{kj}^{mn} are shown as follows:

$$
\begin{aligned}
\frac{\partial \rho_{12}^{mn}}{\partial t} &= -\gamma_{21}\rho_{12}^{mn} - iT_{1+}(t)\sum_{m'n'}\Omega_{1+}(mn,m'n')\rho_{13}^{m'n'} - iT_{1-}(t)\sum_{m'n'}\Omega_{1-}(mn,m'n')\rho_{14}^{m'n'},\\
\frac{\partial \rho_{13}^{mn}}{\partial t} &= -\gamma_{31}\rho_{13}^{mn} - iT_{1+}^{*}(t)\sum_{m'n'}\Omega_{1+}^{*}(mn,m'n')\rho_{12}^{m'n'} - i\Omega_{L+}^{mn*},\\
\frac{\partial \rho_{14}^{mn}}{\partial t} &= -\gamma_{41}\rho_{14}^{mn} - iT_{1-}^{*}(t)\sum_{m'n'}\Omega_{1-}^{*}(mn,m'n')\rho_{12}^{m'n'} - i\Omega_{L-}^{mn*},\\
\frac{\partial \rho_{15}^{mn}}{\partial t} &= -\gamma_{51}\rho_{15}^{mn} - iT_{2+}(t)\sum_{m'n'}\Omega_{2+}(mn,m'n')\rho_{16}^{m'n'} - iT_{2-}(t)\sum_{m'n'}\Omega_{2-}(mn,m'n')\rho_{17}^{m'n'},\\
\frac{\partial \rho_{16}^{mn}}{\partial t} &= -\gamma_{61}\rho_{16}^{mn} - iT_{2+}^{*}(t)\sum_{m'n'}\Omega_{2+}^{*}(mn,m'n')\rho_{15}^{m'n'} - i\Omega_{R+}^{mn*},\\
\frac{\partial \rho_{17}^{mn}}{\partial t} &= -\gamma_{71}\rho_{17}^{mn} - iT_{2-}^{*}(t)\sum_{m'n'}\Omega_{2-}^{*}(mn,m'n')\rho_{15}^{m'n'} - i\Omega_{R-}^{mn*},
\end{aligned}
\tag{11}
$$

where $\Omega_{1(2)\pm}(mn,m'n') = \int dr d\psi \mathcal{L}^{mn*}(r,\psi)R_{1(2)\pm}(r)\mathcal{L}^{m'n'}(r,\psi)$ are coupling coefficients. Apparently, in the present situation, the different $(\mathrm{LG})_n^m$ modes are coupled together. For simplicity, we assume that $R_{1(2)\pm}(r) = \exp[-r^2/w^2]$, where w is the beam waist of the controlling fields, and $T_{1(2)+} = T_0[1 - 0.5\tanh\frac{t-t_1}{t_s} + 0.5\tanh\frac{t-t_2}{t_s} - 0.5\tanh\frac{t-t_3}{t_s} + 0.5\tanh\frac{t-t_4}{t_s}]$ and $T_{1(2)-} = T_0[0.5\tanh\frac{t-t_2}{t_s} - 0.5\tanh\frac{t-t_3}{t_s}]$. Figure 6 shows the retrieval efficiency η of the signal field with the $(\mathrm{LG})_0^1$ mode under different intensity T_0 of the controlling fields by numerical simulation. We can easily see that the nonuniform controlling fields have a significant influence on the retrieval efficiency η. With the increasing of the beam waist w, the nonuniform controlling fields gradually approach to the uniform ones in the interaction location between light fields and atoms, and the obtained results are gradually irrelevant to the spatial distribution of the controlling fields.

Based on the above analysis, a light beam carrying OAMs can also be employed as the controlling fields. However, the

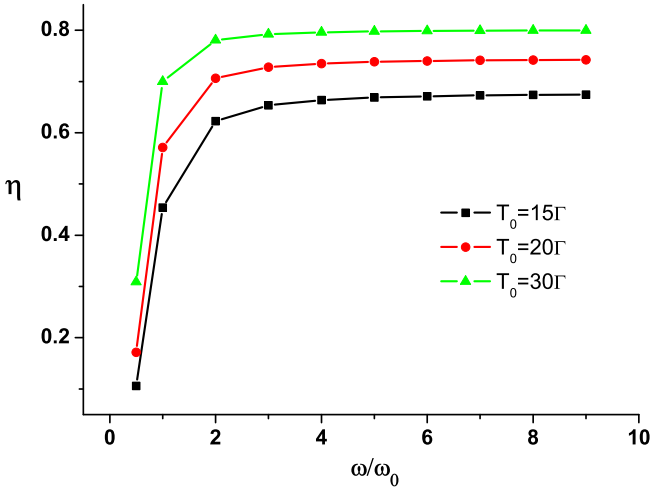

FIG. 6. Retrieval efficiency η of the signal field with the $(LG)_0^1$ mode via the beam waist ratio ω/ω_0 (ω_0 is the beam waist of the signal field) for different maximum intensities T_0 of the controlling fields. The other parameters are the same as in Fig. 2.

EIT will disappear at the vortex core because the intensity of the controlling fields goes to zero in the spatial region. To avoid such absorption losses, an extra controlling field without an optical vortex should be employed in a more complex scheme for guaranteeing that the total intensity of the controlling field is nonzero at the vortex core. Using such schemes, the transfer of the optical vortex from the controlling field to the signal field has been reported [50,51].

IV. CONCLUSIONS

In conclusion, we have proposed an efficient scheme for the reversible storage and manipulation of signal fields encoded in DOFs of polarization and OAM in a double-M system of cold atoms. Analytical analysis shows that the present system exhibits DSPs relating to the polarization and propagation direction of the light fields. As the controlling fields $\Omega_{1\pm}$ ($\Omega_{2\pm}$) are switched on simultaneously, two signal fields with left (right) circular polarization propagating in the opposite directions can be retrieved from the same atomic spin coherence ρ_{12} (ρ_{15}), then the SLPs with polarizations and OAM information can be generated due to their tight coupling and balanced competition. Numerical simulation shows that the SLPs can be manipulated coherently and all-optically by modulating the controlling fields in time adiabatically. Another advantage of our proposed scheme is that the signal fields with left and right circular polarizations can be retrieved independently and can be separated spatially, then the scheme can be employed as a coherent storage-based polarization beam splitter. We believe that such a multiple DOF-dependent scheme with the advantage of tunability and large capacity could pave the way toward quantum nonlinear optics without a cavity, and is promising for practical applications in classical and quantum information processing.

ACKNOWLEDGMENTS

This research was supported by the National Natural Science Foundation of China (Grants No. 11604174, No. 11547035, and No. 61772295) and the Natural Science Foundation of Shandong Province (Grants No. ZR2014AP006 and No. ZR2016FB09).

[1] H. J. Briegel, W. Dur, J. I. Cirac, and P. Zoller, Phys. Rev. Lett. **81**, 5932 (1998).
[2] L. M. Duan, M. D. Lukin, J. I. Cirac, and P. Zoller, Nature (London) **414**, 413 (2001).
[3] D. F. Phillips, A. Fleischhauer, A. Mair, R. L. Walsworth, and M. D. Lukin, Phys. Rev. Lett. **86**, 783 (2001).
[4] Y. F. Hsiao, P. J. Tsai, H. S. Chen, S. X. Lin, C. C. Hung, C. H. Lee, Y. H. Chen, Y. F. Chen, I. A. Yu, and Y. C. Chen, Phys. Rev. Lett. **120**, 183602 (2018).
[5] S. W. Su, Z. K. Lu, S. C. Gou, and W. T. Liao, Sci. Rep. **6**, 35402 (2016).
[6] J. A. Souza, E. Figueroa, H. Chibani, C. J. Villas-Boas, and G. Rempe, Phys. Rev. Lett. **111**, 113602 (2013).
[7] M. Himsworth, P. Nisbet, J. Dilley, G. Langfahl-Klabes, and A. Kuhn, Appl. Phys. B **103**, 579 (2011).
[8] M. Afzelius, C. Simon, H. de Riedmatten, and N. Gisin, Phys. Rev. A **79**, 052329 (2009).
[9] H. de Riedmatten, M. Afzelius, M. U. Staudt, C. Simon, and N. Gisin, Nature (London) **456**, 773 (2008).
[10] K. F. Reim, P. Michelberger, K. C. Lee, J. Nunn, N. K. Langford, and I. A. Walmsley, Phys. Rev. Lett. **107**, 053603 (2011).
[11] K. F. Reim, J. Nunn, V. O. Lorenz, B. J. Sussman, K. C. Lee, N. K. Langford, D. Jaksch, and I. A. Walmsley, Nat. Photonics **4**, 218 (2010).
[12] M. Hosseini, B. M. Sparkes, G. Campbell, P. K. Lam, and B. C. Buchler, Nat. Commun. **2**, 174 (2011).
[13] M. Hosseini, G. Campbell, B. M. Sparkes, P. K. Lam, and B. C. Buchler, Nat. Phys. **7**, 794 (2011).
[14] S. W. Su, S. C. Gou, L. Y. Chew, Y. Y. Chang, I. A. Yu, A. Kalachev, and W. T. Liao, Phys. Rev. A **95**, 061805(R) (2017).
[15] W. T. Liao, C. H. Keitel, and A. Pálffy, Phys. Rev. Lett. **113**, 123602 (2014).
[16] M. Fleischhauer and M. D. Lukin, Phys. Rev. Lett. **84**, 5094 (2000).
[17] C. Liu, Z. Dutton, C. H. Behroozi, and L. V. Hau, Nature (London) **409**, 490 (2001).
[18] H. H. Wang, Y. F. Fan, R. Wang, L. Wang, D. M. Du, Z. H. Kang, Y. Jiang, J. H. Wu, and J. Y. Gao, Opt. Lett. **34**, 2596 (2009).
[19] K. Honda, D. Akamatsu, M. Arikawa, Y. Yokoi, K. Akiba, S. Nagatsuka, T. Tanimura, A. Furusawa, and M. Kozuma, Phys. Rev. Lett. **100**, 093601 (2008).
[20] J. Appel, E. Figueroa, D. Korystov, M. Lobino, and A. I. Lvovsky, Phys. Rev. Lett. **100**, 093602 (2008).
[21] K. S. Choi, H. Deng, J. Laurat, and H. J. Kimble, Nature (London) **452**, 67 (2008).
[22] A. André and M. D. Lukin, Phys. Rev. Lett. **89**, 143602 (2002).
[23] M. Bajcsy, A. S. Zibrov, and M. D. Lukin, Nature (London) **426**, 638 (2003).

[24] A. André, M. Bajcsy, A. S. Zibrov, and M. D. Lukin, Phys. Rev. Lett. **94**, 063902 (2005).
[25] S. A. Moiseev, A. I. Sidorova, and B. S. Ham, Phys. Rev. A **89**, 043802 (2014).
[26] Y. Xue and B. S. Ham, Phys. Rev. A **78**, 053830 (2008).
[27] Y. W. Lin, W. T. Liao, T. Peters, H. C. Chou, J. S. Wang, H. W. Cho, P. C. Kuan, and I. A. Yu, Phys. Rev. Lett. **102**, 213601 (2009).
[28] F. E. Zimmer, J. Otterbach, R. G. Unanyan, B. W. Shore, and M. Fleischhauer, Phys. Rev. A **77**, 063823 (2008).
[29] Y. Zhang, Y. Zhang, X. H. Zhang, M. Yu, C. L. Cui, and J. H. Wu, Phys. Lett. A **376**, 656 (2012).
[30] S. A. Moiseev and B. S. Ham, Phys. Rev. A **73**, 033812 (2006).
[31] Y. H. Chen, M. J. Lee, W. L. Hung, Y. C. Chen, Y. F. Chen, and I. A. Yu, Phys. Rev. Lett. **108**, 173603 (2012).
[32] M. Shuker, O. Firstenberg, R. Pugatch, A. Ron, and N. Davidson, Phys. Rev. Lett. **100**, 223601 (2008).
[33] P. K. Vudyasetu, R. M. Camacho, and J. C. Howell, Phys. Rev. Lett. **100**, 123903 (2008).
[34] G. Heinze, A. Rudolf, F. Beil, and T. Halfmann, Phys. Rev. A **81**, 011401(R) (2010).
[35] A. Mair, A. Vaziri, G. Weihs, and A. Zeilinger, Nature (London) **412**, 313 (2001).
[36] J. Leach, B. Jack, J. Romero, A. K. Jha, A. M. Yao, S. Franke-Arnold, D. G. Ireland, R. W. Boyd, S. M. Barnett, and M. J. Padgett, Science **329**, 662 (2010).
[37] J. W. R. Tabosa and D. V. Petrov, Phys. Rev. Lett. **83**, 4967 (1999).
[38] S. Barreiro and J. W. R. Tabosa, Phys. Rev. Lett. **90**, 133001 (2003).
[39] D. Akamatsu and M. Kozuma, Phys. Rev. A **67**, 023803 (2003).
[40] A. Nicolas, L. Veissier, L. Giner, E. Giacobino, D. Maxein, and J. Laurat, Nat. Photonics **8**, 234 (2013).
[41] Z. Q. Zhou, Y. L. Hua, X. Liu, G. Chen, J. S. Xu, Y. J. Han, C. F. Li, and G. C. Guo, Phys. Rev. Lett. **115**, 070502 (2015).
[42] D. S. Ding, Z. Y. Zhou, B. S. Shi, and G. C. Guo, Nat. Commun. **4**, 2527 (2013).
[43] D. S. Ding, W. Zhang, Z. Y. Zhou, S. Shi, G. Y. Xiang, X. S. Wang, Y. K. Jiang, B. S. Shi, and G. C. Guo, Phys. Rev. Lett. **114**, 050502 (2015).
[44] V. Parigi, V. D'Ambrosio, C. Arnold, L. Marrucci, F. Sciarrino, and J. Laurat, Nat. Commun. **6**, 7706 (2015).
[45] P. C. Humphreys, W. S. Kolthammer, J. Nunn, M. Barbieri, A. Datta, and I. A. Walmsley, Phys. Rev. Lett. **113**, 130502 (2014).
[46] T. S. Yang, Z. Q. Zhou, Y. L. Hua, X. Liu, Z. F. Li, P. Y. Li, Y. Ma, C. Liu, P. J. Liang, X. Li, Y. X. Xiao, J. Hu, C. F. Li, and G. C. Guo, Nat. Commun. **9**, 3407 (2018).
[47] W. Zhang, D. S. Ding, M. X. Dong, S. Shi, K. Wang, S. L. Liu, Y. Li, Z. Y. Zhou, B. S. Shi, and G. C. Guo, Nat. Commun. **7**, 13514 (2016).
[48] D. L. Andrews and M. Babiker, *The Angular Momentum of Light* (Cambridge University, Cambridge, England, 2013).
[49] M. Moos, M. Honing, R. Unanyan, and M. Fleischhauer, Phys. Rev. A **92**, 053846 (2015).
[50] J. Ruseckas, A. Mekys, and G. Juzeliūnas, Phys. Rev. A **83**, 023812 (2011).
[51] J. Ruseckas, V. Kudriašov, I. A. Yu, and G. Juzeliūnas, Phys. Rev. A **87**, 053840 (2013).